Effect of Geometry and Gate Voltage on the Conductance of an Ideal Strip of Graphene

by

Hadi Momtazbaf

A Project Submitted in Partial Fulfillment of the

Requirements for the Degree of

MASTER OF ENGINEERING

in the Department of Electrical and Computer Engineering

April 2015

University of Victoria

Effect of Geometry and Gate Voltage on the Conductance of an Ideal Strip of Graphene

by

Hadi Momtazbaf

Supervisory Committee

Dr. T. Aaron Gulliver, Supervisor
(Department of Electrical and Computer Engineering)

Dr. Tao Lu, Departmental Member
(Department of Electrical and Computer Engineering)

Abstract

One of the enormous challenges in the transistor fabrication industry is to find materials with suitable electronic properties. On the other hand, the size of electronic systems is being reduced every day. Therefore, flexibility and suitable electronic properties are required simultaneously.

Graphene is a perfect example of a two dimensional (2D) electronic transport system that shows resilience, as it is a very specific one-atom thick structure that has surprising metallic electronic properties. In this report, I have simplified the mode-dependent transmission probability of Dirac fermions in an ideal graphene nanoribbon (length *L*, width *W*, and no impurities), to determine the conductance as a function of the Fermi energy in the channel. The conductance results presented in this project are based on two main components (a) geometry, and (b) chemical potential variation in the channel (gate voltage). First by setting the gate voltage to zero, the effect of altering the geometry (aspect ratio between *W* and *L*), on the conductance is evaluated. Then the chemical potential (gate voltage) is changed while keeping the geometry fixed. Finally, the physical relationship between the chemical potential and gate voltage in a field effect transistor (FET) channel is examined, and the connection between the conductance and gate voltage for a range of aspect ratios is assessed.

Performance results are presented which show that the conductance of a narrow and wide graphene strips has a universal minimum value (quantum conductance), at the Dirac point (gate voltage equal to zero), which is an important criterion in achieving a ballistic channel.

Dedication

Dedicated to my loved ones, who inspire me every step of the way.

Contents

List of Figures

Acronyms

1D	One Dimensional
FET	Field Effect Transistor
Si	Silicon
Ge	Germanium
GaAs	Gallium Arsenide
2D	Two Dimensional
SiO_2	Silicon Dioxide
RF	Radio Frequency
W	Width
L	Length
MOSFET	Metal Oxide Semiconductor Field Effect Transistor
GFET	Graphene Field Effect Transistor
QED	Quantum Electro Dynamics
IQHE	Integer Quantum Hall Effect
3D	Three Dimensional
SG	Suspended Graphene
NSG	Non suspended Graphene

1 Introduction

The outstanding electronic and thermal properties of graphene hold great potential for applications in future integrated circuits. Graphene has drawn attention for its transistor applications, first due to its high carrier mobility, i.e. $\sim 104\ cm^2 \cdot V^{-1} \cdot s^{-1}$ [1] and the fact that the electron and hole energy bands are symmetric [1], generating equal and high electron and hole mobility, unlike in typical semiconductors like Si, Ge, or GaAs where hole mobility is lower. Recent work has also identified drift velocity saturation in graphene at values several times higher than in silicon and other common semiconductors [2]. The discovery of graphene introduced a new category of nano electronic devices based on the remarkable physical properties of this one-atom-thick layer of carbon. Unlike two-dimensional electron layers in semiconductors where the charge carriers become immobile at low densities, the carrier mobility in graphene can remain high, even when their density tends to zero at the Dirac point [4].

According to the two well-known experiments [3,4] the conductivity of graphene (a single atomic layer of carbon) has a minimum value on the order of the quantum unit e^2/h when the concentration of carriers is close to zero. This is an intrinsic property of two-dimensional Dirac fermions (charge carriers in a 2D graphene sheet), which can be predicted in an ideal structure without any impurities or lattice defects [5]. Recent measurements in graphene channels show that the noise in these channels is 3 times smaller than in the same geometrical structures with semiconductors due to the elimination of impurity scattering. This is almost identical to the value for a disordered metal [6].

The evaluation of conductance in two-dimensional graphene shows the importance of dimensionality for quantum transport. The evaluation presented in this report was inspired by the work of Tworzydło et al. [7], who used the Landauer transmission formula to calculate the quantum limited conductivity. Using the same approach, a simplification of the transmission probabilities of charge carriers in a graphene strip is given in this report. Due to the importance of the graphene geometry, the transmission probability depends on the aspect ratio W/L of the strip and also on microscopic features of the upper and lower edges. For simplification, the

graphene strip is assumed to be extremely short and wide $\left({}^{w}/_{L} \gg 1\right)$. In this case the microscopic details of the edges become negligible. First the simplest case of a smooth edge, on the scale of the lattice spacing, is considered. Then for a fixed aspect ratio (${}^{w}/_{L}$), the effect of the chemical potential in the channel on the conductivity of the graphene strip is studied. Chemical potential is directly proportional to the charge carrier's concentrations and sometimes it is named as Fermi energy. Finally, according to the relationship between the chemical potential and gate voltage, the influence of gating on the conductivity in graphene transistors for two sets of aspect ratios is evaluated.

2 Background

2.1 Carbon based structures

Carbon is a key element for life on the planet and the basis of all organic chemistry. Flexibility of carbon bonding has made carbon-based systems virtually unlimited in terms of the number of different structures with a vast array of physical and electronic properties. These physical properties are mostly a consequence of the dimensionality of these structures. Among systems with only carbon atoms, graphene, a two-dimensional (2D) structure of carbon, plays a significant role because it is the key to examining the electronic properties of other structures. Graphene is made out of carbon atoms arranged in a hexagonal structure as shown in Fig. 1, and can be considered as composed of benzene rings stripped of their hydrogen atoms. Fullerenes are molecules where the carbon atoms are arranged spherically, and therefore from a physical perspective, are zero-dimensional objects with discrete energy states. Fullerenes can be obtained from graphene by introducing pentagons (which create positive curvature defects), and thus fullerenes can be thought as rolled up graphene.

Carbon nanotubes are made by wrapping graphene in a specific direction and reconnecting the carbon bonds. Thus, carbon nanotubes have only hexagons and can be categorized as one dimensional (1D) objects. Graphite, a three dimensional (3D) allotrope of carbon, is universally known due to the invention of the pencil in 1564. Its practicality as a tool for writing comes from

the fact that graphite is made out of bundles of graphene layers that are weakly held together by van der Waals forces. Thus, when a pencil is pressed on a sheet of paper, graphene bundles are actually being produced and individual graphene layers could be found within them. Although graphene is the parent of all these carbon allotropes and is produced every time a pencil is used for writing, research on graphene only began four centuries after its discovery [8]. The reasons are that it was thought that graphene does not exist in a free state and, even with this knowledge no laboratory instruments existed to observe and fabricate these one-atom-thick structures.

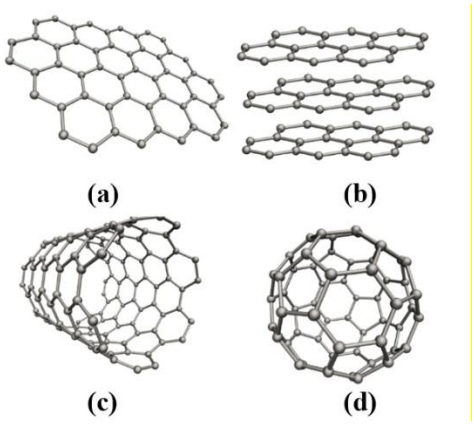

Figure 1. (a) Graphene is a single layer of carbon atoms in a hexagonal lattice. (b) Graphite can be considered a bundle of graphene layers. (c) Carbon nanotubes (CNT) are cylinders of graphene. (d) Fullerenes (C60) are molecules consisting of graphene with pentagons introduced in the hexagonal lattice [9].

Graphene was finally made using an indirect optical technique and an intelligently chosen SiO_2 substrate [8] that makes it observable using an ordinary optical microscope. Hence, graphene is easy to make but not easy to find. The structural flexibility of graphene is reflected in its electronic properties. The $sp2$ hybridization between one $s-orbital$ and two $p-orbitals$ creates a triangular planar structure [10] with a $\sigma-bond$ between carbon atoms which are separated by 1.42 Å. The $\sigma-band$ is responsible for the robustness of the lattice structure in all carbon allotropes. According to the Pauli principle, these bands have a complete shell and therefore create a deep valence band. The unaffected $p-orbital$, which is perpendicular to the planar structure, can bind covalently with neighboring carbon atoms leading to the formation of a $\pi-band$. Because each p-orbital has one extra electron, the $\pi-band$ is half-occupied. Half-occupied bands in transition elements have played a significant role in the physics of heavily

correlated systems [11] because of their tight binding character. As a consequence, their Coulomb energies are very large leading to strong collective effects, magnetism, and insulating behavior due to correlation gaps.

2.2 FET graphene transistors

The key element in wireless communication systems is radiofrequency (RF) transistors that amplify signals to create electronic gain at high frequencies. However, the performance of these transistors decline at high frequencies. Thus, new devices are needed to operate at these frequencies. The cut-off frequency (f_t), and the maximum oscillation frequency (f_{max}), are the two main criteria that determine the frequency performance of a transistor. Utilizing materials with higher charge mobility will improve this performance.

Graphene is considered to be one of the most beneficial materials for the channel in FETs in the near future, as metal–oxide–semiconductor field-effect transistors (MOSFETs) sizes are reduced. The high mobility and excellent chemical and mechanical properties of graphene [12] have resulted in significant research on graphene transistors for RF applications. In the last decade, numerous experimental studies have been conducted on graphene based transistors. Considerable improvements have been made since the introduction of the first high frequency (GHz) graphene transistors [13] in 2008. A graphene FET broke the 100 GHz limit in February 2010, and only a few months later a new graphene FET was created with a cut off frequency of 300 GHz. Meric et al. [14] showed that graphene FETs (GFETs) can be used in radio-frequency circuits.

To facilitate GFET applications, analytic models for the drain current, transconductance, threshold voltage, and cutoff frequency are greatly needed. The drain current model is one of the most important. Thiele et al. [15] used a quasi-analytic modeling approach to calculate the current–voltage (*I*–*V*) characteristics. Jiménez and Moldovan [16] used the drift-diffusion carrier transport approach to obtain an explicit drain current model. Wang et al. [17] presented a virtual-source *I*–*V* model.

The majority of researchers fabricate graphene by mechanical exfoliation, a process developed by the Nobel Prize winners Novoselov and Geim. In this practical method, graphene flakes are peeled off a graphite crystal (the 300 GHz FET mentioned above was made using this method). To make usable graphene on an industrial scale, a process called epitaxy is employed. This approach was introduced by Berger and de Heer using silicon carbide wafers [18]. Chemical vapor deposition is another common method for depositing graphene on a metal and then transferring it onto a silicon substrate with a top layer of silicon dioxide.

2.3 Dirac fermions

One of the most important aspects of graphene is that its low energy excitations are massless, Dirac fermions [19]. In neutral graphene, the Fermi energy (chemical potential) exactly crosses the Dirac point. This property, which is important at low energies, resembles the physics of quantum electrodynamics ($QEDs$) for massless fermions except for the fact that in graphene the Dirac fermions move with a speed v_F which is 300 times less than the speed of light. Therefore, many of the important properties of $QEDs$ can appear in graphene but at considerably lower speeds. Dirac fermions act in an unpredictable manner compared to ordinary electrons if subjected to magnetic fields. This has led to new physical phenomena such as the anomalous integer quantum Hall effect ($IQHE$) which has been measured experimentally by Novoselov et al. and Zhang et al., 2005) [20]. Besides being qualitatively different from the $IQHE$ observed in Si and $GaAlAs$ (hetero structures) devices, the $IQHE$ in graphene can be observed at room temperature because of the large cyclotron energies for "relativistic" electrons Novoselov et al. In other words, the anomalous $IQHE$ is the Dirac fermion behavior.

Another unusual property of Dirac fermions is their blindness to external electrostatic potentials due to the so-called Klein paradox. This means that Dirac fermions can be propagated with probability one through a classically forbidden channel. In fact, Dirac fermions behave in a very unique way in the presence of confining potentials leading to the phenomenon of zitterbewegung (ZB), or jittery motion of the wave function. This motion [21] has attracted the

attention of scientists as this is one of the most interesting phenomena in relativistic quantum physics. Zitterbewegung is a theoretical rapid motion of elementary particles, in particular electrons, that obey the Dirac equation. Zitterbewegung of a free relativistic particle has never been observed. However, the introduction of graphene which is explained by the Dirac equation, has made it the possible to examine ZB approaches.

2.4 Suspended graphene transistors

The excitation energy of massless Dirac fermions in graphene is surprisingly low. This implies unusual electronic properties such as a negative index of refraction [23], specular Andreev reflections at graphene–superconductor junctions [22], and evanescent transport [24]. In addition, graphene as a semimetal can be utilized in nanoscale devices as it maintains its conductivity without becoming an insulator as happens with many doped semiconductors. The explanation behind these properties is that graphene is minimally impacted by interactions with the environment, although the substrate can have a significant influence on these ultrathin films. Carrier mobility is reduced in graphene deposited on silicon/SiO_2 due to trapped charges in the oxide or at the graphene–oxide interface. Moreover, atomic irregularities on the substrate can

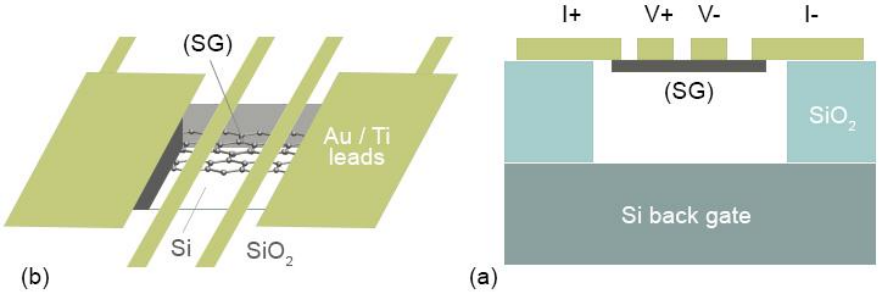

Figure 2. A suspended graphene (SG) sample. (a) Schematic representation of the structure of the SG devices (side view). (b) top view. The electrodes are shown in yellow.

decrease the mobility by creating short-range scattering centers for the graphene layer [25]. Therefore measuring the intrinsic transport properties close to the Dirac point is possible by studying graphene in the absence of a supporting substrate. Eliminating the substrate-induced

perturbations can be achieved by suspending the graphene films from gold/titanium contacts to bridge a channel in a SiO_2 substrate, as shown in Fig. 2a. Initial fabrications of suspended graphene (SG) [26], did not provide electrical contacts for transport measurements. However, the SG device described in this report includes multiple electrodes that allow precise transport measurements. These devices were fabricated from non-suspended graphene (NSG) devices using wet chemical etching [27]. In a regular SG device (shown in Fig. 2b), the graphene layer is suspended from the voltage leads, which run across the sample and simultaneously provide structure. This two-lead configuration avoids complications such as sensitivity to the properties of the lead geometry that arise in ballistic devices when transport measurements are carried out with a conventional design. In two lead arrangements, the measured transport properties of ballistic devices depend on the lead separation and doping, and the calculations can be done in a straightforward way using first principles.

3 GFET Conductance Evaluation

The graphene band structure has two valleys that are separated in the first case by a smooth edge. In a given valley, the excitations have a two-component wave function $\psi = (\psi_1, \psi_2)$ varying on scales that are sufficiently large compared to the lattice spacing. This assumption for

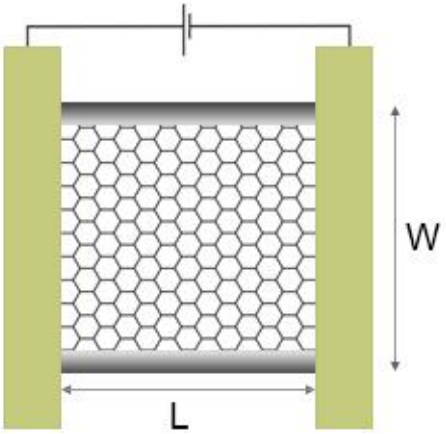

Figure 3. Schematic of a strip of graphene of width *W*, with two electrodes (yellow rectangles) separated by a distance *L*. A voltage source creates a current through the strip.

the wave function has been proved to be quite accurate and it explains the two sub lattices in the graphene lattice structure. In this report, numerical simulation is used to confirm the transmission probability formula. The two components of the wave function ψ introduce the two sub lattices in the two-dimensional hexagonal lattice of graphene. According to the nature of charge transport (Dirac fermions) in graphene, the wave equation for ψ is the Dirac equation

$$\left[\upsilon P_x\sigma_x + \upsilon P_y\sigma_y + \upsilon^2 M(y)\sigma_z + \mu(x)\right]\psi = \varepsilon\psi \qquad (1)$$

where υ is the velocity of the massless excitations of Dirac fermions with energy ε, $P = -i\hbar\partial/\partial r$ the momentum operator, $r = (x, y)$ is the position, and σ_i is the Pauli matrix. The energy is set to zero so that the Fermi level is at $\varepsilon = 0$. Due to the geometry of the graphene strip, the mass term $M(y)$ is zero in the interior of the strip and rises to 1 at the edges $y = 0$ and $y = W$, which confines the particles. As shown by Berry and Mondragon [28], the two components of the wave function should satisfy the boundary conditions at $y = w$ and $y = 0$. As a result, the transversal momenta are quantized as

$$q_n = 1/w\,\pi\,(n + 1/2)\,; \qquad n = 0,1,2,\ldots \qquad (2)$$

where n is the propagation mode. The chemical potential (Fermi energy in the graphene channel), is $\mu(x) = \mu$ for $0 < x < L$. This can be varied by a gate voltage and determines the concentration of the charge carriers in the strip. The neutral graphene value $\mu = 0$ is related to the point where electron and hole excitations are degenerate (known as the Dirac point). In these results obtained by J. Tworzydło, the drain and source electrodes are modeled by taking a large value $\mu(x) = \mu_\infty$ for the leads at $x < 0$ and $x > L$ [29].

The transmission probabilities at the Fermi level can be calculated by mode matching at $x = 0$ and $x = L$. For the Dirac equation, the continuity of the two components of ψ is the only matching condition because this provides the current density conservation, and the continuity of the derivatives is not required (as with the Schrodinger equation). This matching condition does not mix modes, so there are n separate transmission probabilities for each of the *N* propagation

modes T_n in the graphene channel. The details of the mode matching calculations can be found in [30]. These results are continued in this project. At the Dirac point $\mu = 0$, the transmission probability is

$$T_n = \left| \frac{k_n}{k_n \cos(k_n L) + i\left(\frac{\mu}{\hbar v}\right)\sin(k_n L)} \right|^2 \qquad (3)$$

$$k_n = \sqrt{(\mu/\hbar v)^2 - q_n^2}$$

The conductance *G* can be obtained by summing over the modes

$$\mathrm{G} = G_0 \sum_{n=0}^{N-1} T_n \qquad (4)$$

with $G_0 = 4e^2/h$. The dependence of the conductivity $\sigma = G \times L/W$ on the aspect ratio W/L shows the importance of the geometry on graphene conductivity. In order to evaluate (4), the transmission probabilities in (3) should be rewrtitten so that the aspect ratio W/L is separate

$$T_n = \frac{k_n^4 \cos^2(k_n L) + k_n^2 (\mu/\hbar v)^2 \sin^2(k_n L)}{[k_n^2 \cos^2(k_n L) + i\left(\frac{\mu}{\hbar v}\right)^2 \sin^2(k_n L)]^2} \qquad (5)$$

$$k_n = \sqrt{(\mu/\hbar v)^2 - q_n^2}\ , \quad For\ \mu \to 0 :\ k_n = i\sqrt{q_n^2} \qquad (6)$$

Using (6), in the absence of chemical potential ($\mu \to 0$), the transmission probability for Dirac fermions in the graphene channel is

$$T_n = \frac{1}{\cosh^2(q_n L)} \qquad (7)$$

According to (4) the conductance *G* can be achieved by summing over the modes, and using the aspect ratio of the graphene strip, the conductivity of the graphene sheet for the condition ($\mu \rightarrow 0$) is

$$\sigma = G \times L/w \qquad \mathrm{G} = G_0 \sum_{n=0}^{N-1} T_n \qquad (8)$$

Equation (7) can be considered as the conductivity formula when the graphene transistor is OFF and the gate voltage is close to zero ($V_G = 0$). The conductivity when the graphene transistor is ON can be calculated using the transmission probability formula for $\mu \neq 0$. In this case, the chemical potential (μ) terms in T_n cannot be ignored, so the simplification must be carried out in multiple steps. Starting with (5), for $\mu \neq 0$ the phase term ($k_n L$) for cos and sin will be complicated. Hence, to simplify the conductivity expression, first $k_n L$ is calculated

$$k_n \mathrm{L} = \sqrt{(\mu/\hbar\upsilon)^2 - q_n^2}\mathrm{L} \qquad (9)$$

Then substituting q_n from (2) into (8), the aspect ratio term (W/L) which is fixed in this step can be separated to obtain

$$k_n \mathrm{L} = \frac{1}{w/L}\sqrt{(\mathrm{w}\mu/\hbar\upsilon)^2 - (\pi/w(n+1/2))^2} \qquad (10)$$

To evaluate the conductivity for a moderate aspect ratio, $^{w}/_{L}$ is set to 5 and x substituted for $\mathrm{w}\mu/\hbar\upsilon$ to further simplify the expression. Then (9) as a function of x and n is

$$k_n \mathrm{L} = {}^{1}/_{5}\sqrt{f(x,n)} \qquad (11)$$

$$f(x,n) = x^2 - \pi^2(n+1/2)^2 \qquad (12)$$

Using $f(x,n)$, the simplified terms for ${k_n}^4$ and ${k_n}^2$ are

$$k_n = \sqrt{(\mu/\hbar\upsilon)^2 - q_n^2} \tag{13}$$

$$k_n{}^2 = \frac{1}{w}\left[(\mathrm{w}\mu/\hbar\upsilon)^2 - (\pi/W(n+1/2))^2\right] \tag{14}$$

$$k_n{}^2 = \frac{f(x,n)}{w^2} \quad , \quad k_n{}^4 = \frac{f(x,n)^2}{w^4} \tag{15}$$

Substituting (10) and (14) in (5), the transmission probability T_n for the ON mode of the graphene transistor ($\mu \neq 0$) is obtained. Thus, the conductivity with a channel aspect ratio of $^{W}/_{L} = 5$ is

$$T_n = \frac{f^2\cos^2\left(\frac{\sqrt{f}}{5}\right) + x^2 f\sin^2\left(\frac{\sqrt{f}}{5}\right)}{\left[\ f\cos^2\left(\frac{\sqrt{f}}{5}\right) + x^2\sin^2\left(\frac{\sqrt{f}}{5}\right)\ \right]^2} \qquad \sigma = G_0/5\sum_{n=0}^{N-1} T_n \tag{16}$$

4 Evaluation Results

To evaluate the analytical results for the transmission probability in the graphene channel, numerical simulations were conducted using (8) and (16) to examine the dependence of the conductance on the aspect ratio W/L of the graphene strip as well as chemical potential in the channel using a hexagonal lattice with metallic armchair edges. A total of 4×10^4 hexagons for the graphene strip were considered, limited on both sides with two infinite leads. The simulation results shown in Figs. 4 and 5 agree with the theoretical predictions for the behavior of charge carriers in a graphene strip.

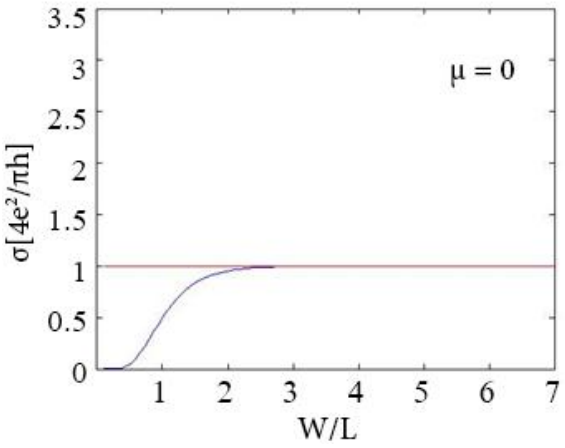

Figure 4. Conductivity $\sigma = G \times L/W$ at the Dirac point (μ = 0), as a function of the aspect ratio of the graphene strip. The curve is plotted using (6) in the limit $N \to \infty$ for smooth and ‘‘metallic armchair’’ edges. The limit $W/L \to \infty$ (red line) is given by (12) for any boundary conditions.

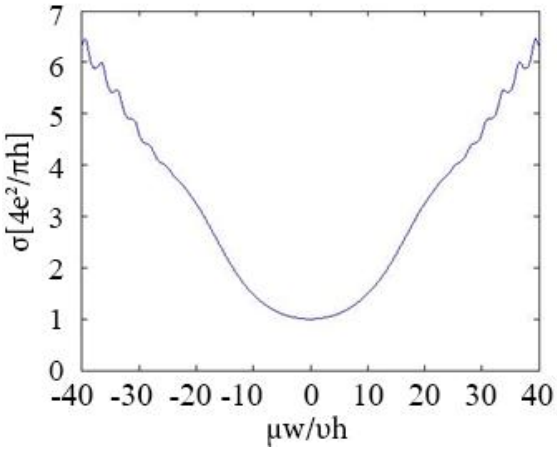

Figure 5. Chemical potential dependence of the conductivity for a fixed aspect ratio $W/L = 5$. The conductivity has a minimum at the Dirac point. The curve is plotted using (11) for the case of a smooth edge.

Figure 4 shows that there is a limiting behavior for the conductivity at the Dirac point ($\mu = 0$) which keeps the values less than $G_0 = 1.54 \times 10^{-5}$. Attaining a minimum conductivity for short and wide graphene strips at the Dirac point indicates that in the absence of chemical potential (gate voltage), that creates a carrier density in the channel, a wider and shorter geometry increases the conductivity up to a constant value of $\sigma_0 = G_0/\pi$ ($^{W}/_{L} \to \infty$, $\sigma \to {}^{g_0}/_{\pi}$). This result has already been achieved for aspect ratios around $W/L = 3$ which very close to the experimental results proposed by Tworzydlo et al [25]. In this project, the limiting behavior was derived only for ideal smooth edge boundary conditions, but from [29] it is clear that this result is universal, as the same results have been reported for more general boundary conditions at the edges of the graphene strip.

Figure 5 illustrates the dependence of the conductance on μ at a fixed value of $W/L = 5$. This shows that the conductivity of a sufficiently short and wide graphene strip is increased by altering the chemical potential μ in the channel. This result is also in agreement with the theoretical predictions. Chemical potential in the channel is proportional to the concentration of the charge carriers in the graphene strip. A higher concentration of carriers increases the

probability of charge transport between the two leads. Thus for a fixed aspect ratio, increasing the transmission probability T_n directly corresponds to an increase in conductivity. In addition, the limiting conductivity behavior is again observed when the concentration of charge carriers (Dirac fermions) goes to zero in the absence of chemical potential at Dirac point ($\mu = 0$).

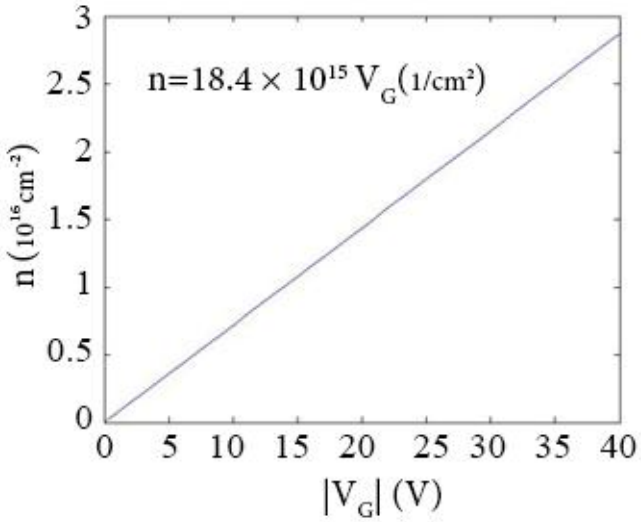

Figure 6. Dependence of the charge carrier density on the gate voltage. The thickness of the oxide layer is $t_{ox} = 300\,nm$. The parameters are $n_G = C_{ox}V_G/q$, capacitance of the oxide layer $C_{ox} = 0.115 \times 10^{-3}F$, and the charge of each carrier $q = 1.6 \times 10^{-3}C$.

According to $\mu = h\nu\sqrt{\pi n_G}$ [30], chemical potential in a graphene field effect transistor (GFET) channel is proportional to the gate voltage induced by the concentration of charge carriers n_G. Using the expression for the carrier concentration in a typical FET channel $n_G = C_{ox}V_G/q$, the effective chemical potential is

$$\mu = h\nu\sqrt{\pi C_{ox}V_G/q}\ , \quad C_{ox} = \varepsilon_{ox}/t_{ox} \qquad (17)$$

where $C_{ox}\ is$ the capacitance of the SiO_2 layer, $\varepsilon_{ox} = 34.3 \times 10^{-14}\,Fcm^{-1}\ is$ the permittivity of SiO_2, $t_{ox} = 300\,nm$ is the thickness of the oxide layer, V_G is the gate voltage and $\upsilon = 10^6\,m/s$ is the velocity of the charge carriers. Figure 6 shows the dependence of the charge carrier concentration on the gate voltage in a graphene channel. For the geometry used in this simulation, the carrier concentration attains $n_G = 71.87 \times 10^{14}cm^{-2}$ for a moderate gate

voltage of $V_G = 10V$. As expected from (17), the charge carrier concentration increases linearly with the gate voltage (as shown in Figure 6). Thus, the chemical potential through the graphene channel can be directly controlled by gating. Using (17) and (4) for the gate voltage and transmission probability, respectively, the dependence of the conductivity on the gate voltage can be simplified to

$$f = V_G - B^2(n + 1/2)^2 , \quad \text{A} = \pi C_{ox}/q \quad B = {}^{\pi}/_{W} \qquad (19)$$

$$T_n = \frac{f^2 \cos^2\left(\sqrt{f}\, L\right) + AV_G\, f \sin^2\left(\sqrt{f}\, L\right)}{\left[\ f \cos^2\left(\sqrt{f}\, L\right) + AV_G \sin^2\left(\sqrt{f}\, L\right)\ \right]^2} \qquad (20)$$

$$\sigma = G_0 L/W \sum_{n=0}^{N-1} T_n \qquad (21)$$

To determine for the effect of the gate voltage on conductivity, numerical simulations were conducted using (20) and (21) for two sets of samples. Each set contains six graphene strips with the same length but different widths. Sets A and B have lengths 1 μm and 0.1 μm, respectively, with widths $5, 2, 1, 0.5, 0.1$ and $0.01\ \mu m$. The thickness of the oxide layer (SiO_2) was $t_{ox} = 300\ nm$ and the capacitance of this layer is $C_{ox} = 0.15 \times 10^{-3}\ Fm^{-2}$. Using (21) and the calculated value of $\text{A} = 2.25 \times 10^{15}$ from (19), the conductance was evaluated for these sets of graphene strips. The reason for using two sets of strips was to examine the effect of both gate voltage and geometry on the conductivity. This will provide a better engineering viewpoint on the parameters associated with conductivity in graphene based field effect transistors.

Figures 7 and 8 give the dependence of the conductivity on the gate voltage for lengths $L1 = 1\ \mu m\ and\ L2 = 0.1\ \mu m$ (sets A and B, respectively), and six different widths (each width is indicated with a different color). The set A samples are an order of magnitude shorter than the Set B samples and the applied gate voltage was in the range of $|V_G| < 40$. These figures show that the behavior is very similar to the chemical potential μ curve in Figure 5. The Minimum point for all curves is at the Dirac point where the concentration of charge carriers is close to

zero due to the absence of a gate voltage. According to the theoretical predictions, ballistic transport can be achieved when the conductivity reaches its minimum value of $\sigma_0 = G_0/\pi$. This minimum conductivity $(\sigma_0 = G_0/\pi)$, can be considered as an indication of approaching to the ballistic transport in any nanoscale system at the Dirac point. This is the reason that in Figures 7 and 8, the conductivity (vertical axis σ) was normalized by $\sigma_0 = 15.4 \times 10^{-5}$. Thus, determining the minimum normalized conductance for a given aspect ratio (W/L) is important because if it is close to 1, the device is ballistic.

In Figure 8, $\sigma(V_G)$ curves were obtained for six different widths in order to find the best aspect ratio for approaching ballistic transport. Minimum conductivity saturation occurs at the widths larger than $W = 1\,\mu m$ and the behavior of the curves is very similar close to the Dirac point. Looking at the corresponding $\sigma(V_G)$ curves for Set B in Figure 8 with $L_2 = 1\,\mu m$, the minimum conductivity points are shifted considerably from $\sigma(V_G) = 1$ which is the reference point for ballistic behavior. The difference between the $\sigma(V_G)$ curves for Set B is much greater than the corresponding curves for Set A. For example, the difference in the minimum conductivity for the red curves which correspond to $W = 100\,nm$ is 10 times greater with the longer length of $L_1 = 100\,nm$. Results from the first simulation step show that for sufficiently wide and short graphene strips, the minimum conductivity is similar to that in Figures 5.

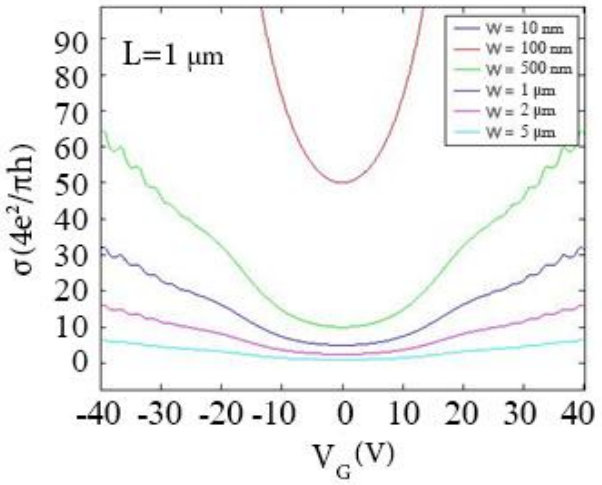

Figure 7. (SET B) gate voltage dependence on the conductivity for 6 different aspect ratios. The length is fixed at $L = 1$ micron. The results were obtained using (21) for the case of a smooth and metallic armchair edge.

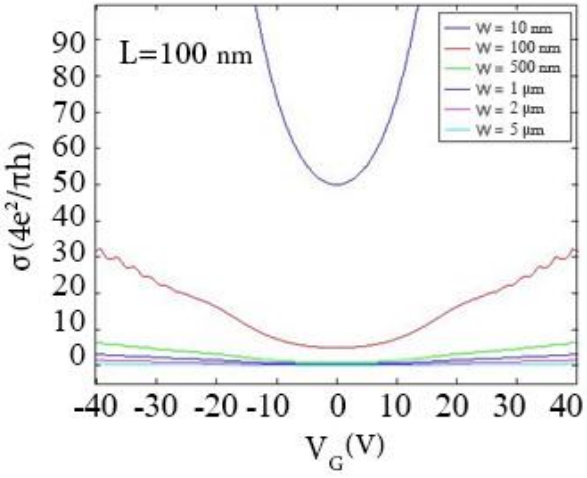

Figure 8. (SET A) gate voltage dependence on the conductivity for 6 different aspect ratios. The length is fixed at $L = 100\,nm$. The results were obtained using (21) for the case of a smooth edge.

In order to use graphene as a channel material in FETs, the charge carrier density must be controlled by the gate voltage. This gating affects the conductivity of the strip significantly to create the ON and OFF modes in GFET transistors. The conductivity of sample sets A and B used in this simulation increased substantially with changes in the forward $(V_G > 0)$ and backward $(V_G < 0)$ gate voltages. Figure 8 illustrates that, for a given gate voltage range $(|V_G| < 40)$ the shorter and wider graphene strips need a higher gate voltage to obtain the same conductivity as the longer samples. For example, by applying a $10\,V$ gate voltage $(V_G = 10\,V)$ on the graphene strip with $L = 1\ \mu m\ and\ W = 100\,nm$, the conductivity is $70\,S$, which is 7 times higher than the conductivity for $L = 100\,nm\ and\ W = 100nm$. This implies that a short and wide geometry could be an advantage for approaching ballistic transport at the Dirac point $(V_G = 0\,V)$. Further, a higher gate voltage can be applied to increase the conductivity of the graphene strip and increase the charge carrier concentration. In addition, Figures 7 and 8 show that the conductivity fluctuates slightly at higher gate voltages. This oscillatory behavior is due to the scattering in the graphene lattice as well as the SiO_2 substrate. Although, substrate induced long range scattering can be neglected by using suspended graphene (SG) samples, a higher gate voltage increases the probability of impurity induced short range scattering through the graphene lattice. Hence, from an engineering perspective a moderate aspect ratio $({}^{W}/_{L} \approx 3)$ is a good choice for GFET devices. This will keep the device close to the minimum conductivity point in order to satisfy the OFF mode conditions of the transistor and increase the gating induced conductivity of the channel to maintain the ON mode of the graphene transistor.

4 Conclusion and future work

Conductivity and transport simulations were conducted for graphene strips. These results indicate that there is a limiting behavior for the conductivity of a graphene strip at the Dirac point $(\mu = 0)$ which keeps the conductivity less that $G_0 = 1.54 \times 10^{-5}$. To achieve this

minimum conductivity at the Dirac point in the absence of a gate voltage, a wider and shorter geometry increases the conductivity up to a constant value $\sigma_0 = G_0/\pi$ ($^{W}/_{L} \to \infty$, $\sigma \to {}^{g_0}/_{\pi}$). The conductivity of graphene strips increases sharply with gate voltage. Shorter aspect ratios require considerably higher gate voltages to obtain the same conductivity as longer geometries. However, at the Dirac point a shorter and wider structure can be considered as an advantage in terms of approaching ballistic transport in graphene.

Future works to extend this study can be done by considering the phonon scattering at different temperature ranges. Given the fact that, graphene problem is being studied mostly in physics, utilizing the graphene as a channel material in FET it requires further researches considering temperature changes as an important factor in conductivity measurements. Frequency response is another point that can be added to this study. Using an AC grate voltage can create different conductivities in different frequency ranges. Therefore, examining the conductivity variation of the graphene by AC gating can be considered as another area for further research.

4 References

[1] Anonymous Graphene: An emerging electronic material. *Adv Mater 24(43),* pp. 5776. 2012.

[2] Anonymous Atomic layer etching of graphene for full graphene device fabrication. *Carbon 50(2),* pp. 429. 2012.

[3] Anonymous New findings from A. novoselov and co-authors describe advances in optical research. *Technology Business Journal* pp. 226. 2010.

[4] M. V. Berry and R. J. Mondragon. Neutrino billiards: Time-reversal symmetry-breaking without magnetic fields. *Proceedings of the Royal Society of London.Series A, Mathematical and Physical Sciences 412(1842),* pp. 53-74. 1987.

[5] J. Chauhan and J. Guo. High-field transport and velocity saturation in graphene. *Appl. Phys. Lett. 95(2),* pp. 023120-023120-3. 2009. DOI: 10.1063/1.3182740.

[6] C. Chen and J. Hone. Graphene nanoelectromechanical systems. *Proc IEEE 101(7),* pp. 1766-1779. 2013. DOI: 10.1109/JPROC.2013.2253291.

[7] J. Chen, W. G. Cullen, C. Jang, M. S. Fuhrer and E. D. Williams. Defect scattering in graphene. *Phys. Rev. Lett. 102(23),* pp. 236805. 2009. DOI: 10.1103/PhysRevLett.102.236805.

[8] D. K. Ferry. Short-range potential scattering and its effect on graphene mobility. *Journal of Computational Electronics 12(2)*, pp. 76-84. 2013. DOI: 10.1007/s10825-012-0431-x.

[9] A. H. C. Neto, F. Guinea, N. M. R. Peres, K. S. Novoselov and A. K. Geim. The electronic properties of graphene. Reviews of Modern Physics 81(1), pp. 109-162. 2009; 2007. DOI: 10.1103/RevModPhys.81.109.

[10] I. V. Grigorieva, D. Jiang, K. S. Novoselov, A. K. Geim, S. V. Dubonos, S. V. Morozov, M. I. Katsnelson and A. A. Firsov. Two-dimensional gas of massless dirac fermions in graphene. *Nature 438(7065)*, pp. 197-200. 2005. DOI: 10.1038/nature04233.

[11] I. F. Herbut. Theory of integer quantum hall effect in graphene. *Physical Review B 75(16)*, 2007; 2006. DOI: 10.1103/PhysRevB.75.165411.

[12] J. A. Jaszczak, K. S. Novoselov, A. K. Geim, F. Schedin, S. V. Morosov, M. I. Katsnelson and D. Elias. Giant intrinsic carrier mobilities in graphene and its bilayer. *Phys. Rev. Lett. 100(1)*, pp. 016602. 2008; 2007. DOI: 10.1103/PhysRevLett.100.016602.

[13] J. Li, L. Niu, Z. Zheng and F. Yan. Photosensitive graphene transistors. *Adv Mater 26(31)*, pp. 5239-5273. 2014. DOI: 10.1002/adma.201400349.

[14] F. Liu, C. Hsu, S. Lo, C. Chuang, L. Huang, T. Woo, C. Liang, Y. Fukuyama, Y. Yang, R. E. Elmquist, P. Wang and X. Lin. Thermometry for dirac fermions in graphene. *Journal of the Korean Physical Society 66(1)*, pp. 1-6. 2015. DOI: 10.3938/jkps.66.1.

[15] H. Lv, H. Wu, J. Liu, J. Yu, J. Niu, J. Li, Q. Xu, X. Wu and H. Qian. High carrier mobility in suspended-channel graphene field effect transistors. *Appl. Phys. Lett. 103(19)*, pp. 193102-193102-4. 2013. DOI: 10.1063/1.4828835.

[16] R. Mas-Ballesté, C. Gómez-Navarro, J. Gómez-Herrero and F. Zamora. 2D materials: To graphene and beyond. *Nanoscale 3(1)*, pp. 2-3. 2011. DOI: 10.1039/c0nr00323a.

[17] R. Maurand, P. Rickhaus, P. Makk, S. Hess, E. Tóvári, C. Handschin, M. Weiss and C. Schönenberger. Fabrication of ballistic suspended graphene with local-gating. *Carbon 79*pp. 486-492. 2014. DOI: 10.1016/j.carbon.2014.07.088.

[18] P. K. Mohseni, A. Behnam, J. D. Wood, C. D. English, J. W. Lyding, E. Pop and X. Li. InxGa1–xAs nanowire growth on graphene: Van der waals epitaxy induced phase segregation. *Nano Letters 13(3)*, pp. 1153-1161. 2013. DOI: 10.1021/nl304569d.

[19] R. Raimondi, P. Schwab and T. Lück. Electronic thermal conductivity of disordered metals. *Physical Review B 70(15)*, 2004. DOI: 10.1103/PhysRevB.70.155109.

[20] T. Toyoda and C. Zhang. Theory of the integer quantum hall effect in graphene. Physics Letters A 376(4), pp. 616-619. 2012. DOI: 10.1016/j.physleta.2011.11.051.

[21] Z. Shen and L. Liu. Bandgap engineering of graphene: A density functional theory study. *Appl. Phys. Lett. 95(25),* pp. 252104-252104-3. 2009. DOI: 10.1063/1.3276068.

[22] K. V. Sreekanth, A. De Luca and G. Strangi. Negative refraction in graphene-based hyperbolic metamaterials. *Appl. Phys. Lett. 103(2),* pp. 023107-023107-4. 2013. DOI: 10.1063/1.4813477.

[23] D. Tománek. Carbon-based nanotechnology on a supercomputer. *Journal of Physics: Condensed Matter 17(13),* pp. R413-R459. 2005. DOI: 10.1088/0953-8984/17/13/R01.

[24] M. Topsakal, V. M. K. Bagci and S. Ciraci. Current-voltage (I-V) characteristics of armchair graphene nanoribbons under uniaxial strain. *Physical Review B 81(20),* 2010. DOI: 10.1103/PhysRevB.81.205437.

[25] J. Tworzydło, B. Trauzettel, M. Titov, A. Rycerz and C. W. J. Beenakker. Sub-poissonian shot noise in graphene. *Phys. Rev. Lett. 96(24),* pp. 246802. 2006. DOI: 10.1103/PhysRevLett.96.246802.

[26] H. Wang, A. Hsu, J. Kong, D. A. Antoniadis and T. Palacios. Compact virtual-source current-voltage model for top- and back-gated graphene field-effect transistors. *IEEE Trans. Electron Devices 59(5),* pp. 1523-1533. 2011. DOI: 10.1109/TED.2011.2118759.

[27] A. Wiener and M. Kindermann. Signatures of evanescent mode transport in graphene. *Physical Review B 84(24),* 2011. . DOI: 10.1103/PhysRevB.84.245420.

[28] H. Xu and T. Heinzel. Selective andreev reflection tuned by magnetic barriers in graphene-superconductor hybrid junctions. *Physics Letters A 377(43),* pp. 3148. 2013.

[29] J. Tworzydło, B. Trauzettel, M. Titov, A. Rycerz and C. W. J. Beenakker. Sub-poissonian shot noise in graphene. Phys. Rev. Lett. 96(24), pp. 246802. 2006. DOI: 10.1103/PhysRevLett.96.246802.

[30] S. Yiğen, V. Tayari, J. O. Island, J. M. Porter and A. R. Champagne. Electronic thermal conductivity measurements in intrinsic graphene. 2013. DOI: 10.1103/PhysRevB.87.241411.